IHEP 2002-16

Measurement of the Dalitz plot slope parameters for $K^- \to \pi^0 \pi^0 \pi^-$ decay using ISTRA+ detector

I.V. Ajinenko, S.A. Akimenko, G.I. Britvich, I.G. Britvich, K.V. Datsko, A.P. Filin, A.V. Inyakin, A.S. Konstantinov, V.F. Konstantinov, I.Y. Korolkov, V.M. Leontiev, V.P. Novikov, V.F. Obraztsov, V.A. Polyakov, V.I. Romanovsky, V.I. Shelikhov, N.E. Smirnov, O.G. Tchikilev, V.A. Uvarov, E.V. Vlasov, O.P. Yushchenko.

Institute for High Energy Physics, Protvino, Russia

V.N. Bolotov, S.V. Laptev, A.R. Pastsjak, A.Yu. Polyarush, A.S. Sadovski, R.Kh. Sirodeev.

Institute for Nuclear Research, Moscow, Russia

Abstract

The Dalitz plot slope parameters g, h and k for the $K^- \to \pi^0\,\pi^0\,\pi^-$ decay have been measured using in-flight decays detected with the "ISTRA+" setup operating in the 25 GeV negative secondary beam of the U-70 PS. About 214K events with four-momenta measured for the π^- and for at least three involved photons were used for the analysis. The values obtained

$$g = 0.697 \pm 0.007(stat) \pm 0.019(syst),$$
$$h = 0.124 \pm 0.007(stat) \pm 0.035(syst),$$
$$k = 0.006 \pm 0.002(stat) \pm 0.004(syst),$$

are consistent with the world averages dominated by K^+ data. Our g value is by 4 standard deviations different from that obtained by previous K^- experiment.

1 Introduction

The determination of the Dalitz plot slope parameters for the $K^{\pm} \to (3\pi)^{\pm}$ decays is of interest as a check on the selection rule $\Delta I = \frac{1}{2}$ and on the direct CP violation. The latter would manifest itself by the difference between the K^+ and K^- decay matrix elements if there are at least two amplitudes with different "weak" phases and different "strong" final state interaction phases (see for example [1]).

The square of the matrix element of the τ' ($K^{\pm} \to \pi^0\pi^0\pi^{\pm}$) decay can be written as

$$|A(K^{\pm} \to 3\pi)|^2 \;\propto\; 1 + g\,Y + h\,Y^2 + k\,X^2 + \ldots\,, \tag{1}$$

where $X = (s_1 - s_2)/m_\pi^2$ and $Y = (s_3 - s_0)/m_\pi^2$ are the Dalitz variables, and the parameters $g \div k$ are the "Dalitz plot slopes". Here $s_i = (p_K - p_i)^2$, $s_0 = \frac{1}{3}(s_1 + s_2 + s_3)$, p_K and p_i are the $K^{\pm}$ and π_i four-momenta (π_3 is the odd pion).

Considering only the linear slopes g^+ and g^-, used in the conventional parameterization (1) for $|A|^2$ in the $K^+ \to \pi^0\pi^0\pi^+$ and $K^- \to \pi^0\pi^0\pi^-$ transitions, the direct CP violation could be detected by the observation of the following charge asymmetry:

$$(\delta g)_{\tau'} = \frac{g^+ - g^-}{g^+ + g^-}. \tag{2}$$

The theoretical predictions for the asymmetry $(\delta g)_{\tau'}$ in the framework of the Standard Model (SM) were originally spread in the wide range of $\sim 2 \cdot 10^{-6} \div 10^{-3}$ [2]. Over last years they have converged to the value of $\sim 10^{-5}$ [1, 3]. In a wide class of possible supersymmetric extensions of the SM, where CP-violating observables do not depend on the phases of the Cabibbo–Kobayashi–Maskawa matrix, larger values are possible. For example, in the Weinberg model [4], where the origin of the CP violation comes from the sector of the scalar fields incorporating more than two Higgs doublets, the value of $\sim 2 \cdot 10^{-4}$ is predicted [5].

This topic has been attracting significant interest during last years. The comparison of the results of the latest K^+ experiment [6] with the only one existing K^- measurement [7] leads to the value of $(\delta g)_{\tau'} = 0.1 \pm 0.02$, i.e. 5 sigma effect. This observation encourages us to perform a new measurement of the Dalitz plot slope parameters g, h and k for the $K^- \to \pi^0\,\pi^0\,\pi^-$ decay, based on the statistics of about 214K events.

2 Experimental setup

The experiment is performed at the IHEP proton synchrotron U-70 with the experimental apparatus "ISTRA+" which is a modification of the "ISTRA-M" setup [8] and described in some details in our recent papers [9], where studies of the K^-_{e3} and $K^-_{\mu 3}$ decays have been presented. The setup is located in the negative unseparated secondary beam with the following parameters in the measurements: the momentum is ~ 25 GeV/c with $\Delta p/p \sim 2\,\%$, the admixture of kaons is $\sim 3\,\%$, and the total intensity is $\sim 3 \cdot 10^6$ per spill.

The schematic layout of the "ISTRA+" detector is shown in Fig. 1. The momentum of the beam particle, deflected by the magnet M1, is measured with four proportional chambers BPC1–BPC4. The kaon identification is done by three threshold gas Cherenkov counters Č1–Č3. The momenta of the secondary charged particles, deflected by the magnet M2, are measured with three proportional chambers PC1–PC3, with three

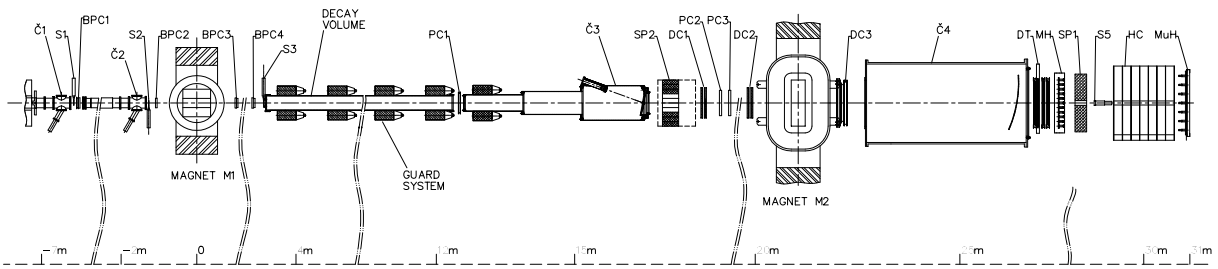

Figure 1: The layout of the "ISTRA+" setup.

drift chambers DC1–DC3, and with four planes of drift tubes DT. The secondary photons are registered by the lead glass electromagnetic calorimeter SP1. To veto low energy photons the decay volume is surrounded by the guard system of eight lead glass rings and by the lead glass calorimeter SP2. The wide aperture threshold helium Cherenkov counter Č4 is used to trigger the electrons. In Fig. 1, HC is a scintillator-iron sampling hadron calorimeter, MH is a scintillator hodoscope used to solve the reconstruction ambiguity for multitrack events and improve the time resolution of the tracking system, MuH is a muon hodoscope.

The trigger is provided by the scintillation counters S1–S5, the Cherenkov counters Č1–Č3, and the sum of the amplitudes from the last dinodes of the calorimeter SP1 (see Ref. [9] for details). The latter serves to suppress the $K^- \to \mu^- \bar{\nu}_\mu$ decay.

3 Event selection

About 206M and 363M events were collected during two physics runs in November–December 1999 and March–April 2001. These experimental data are supported by about 100M events generated with the Monte Carlo program Geant3 [10]. The Monte Carlo simulation includes the realistic description of the experimental setup: the decay volume entrance windows, the track chamber windows, gas, sense wires and cathode structures, the Cherenkov counter mirrors and gas, the showers development in the electromagnetic calorimeters, etc. The details of the reconstruction procedure have been presented in Ref. [9], here only key points relevant to the $K^- \to \pi^-\pi^0\pi^0$ event selection are described.

The data processing starts with the beam particle reconstruction in the proportional chambers BPC1–BPC4, and then with the secondary tracks reconstruction in the tracking system PC1–PC3, DC1–DC3 and DT. Finally, the electromagnetic showers are looked for in the calorimeter SP1. The method of the photons reconstruction is based on the Monte Carlo generated patterns of showers. To suppress leptonic decays of kaons the particle identification is used [9]. The muons are identified using the information from the calorimeters SP1 and HC. The electrons are identified using the ratio of the energy of the shower, detected in the SP1 and associated with the track of the electron, and the momentum of the electron.

In the first step of the event selection only the measurements of the beam and secondary charged particles are used. Those events are selected which satisfy the following requirements:

– only one beam track and only one negative secondary track are detected;

– the probability of the vertex fit, $CL(\chi^2)$, is more than 0.01;

– the decay vertex is in the region before the calorimeter SP2, and its transverse deviation from the setup axis is less than 10 cm;

– the secondary track is associated with the hit in the hodoscope MH when the decay vertex is in the region between the proportional chamber PC1 and the Cherenkov counter Č3;

– the angle between the beam and secondary tracks is more than 1.5 mrad;

– the transverse momentum of the secondary track with respect to the beam direction is less than 150 MeV/c;

– the secondary track is not identified as an electron or as a muon.

In the second step of the event selection the measurements of the showers in the calorimeter SP1 are used. The following requirements are used to choose the photons (showers):

– the distance between the shower and the intersection of the secondary track with the transverse plane of the calorimeter SP1 is more than 9 cm;

– the photon energy is more than 0.7 GeV, but is more than 1.4 GeV when the photon is detected in three or less cells of the calorimeter SP1;

– for events where the secondary track is not associated with any shower in the calorimeter SP1 and with any hit in the hodoscope MH the photon energy is more than 1.4 GeV;

– the energy of the photon found in the multishower cluster is more than 2 GeV.

For each selected $\gamma\gamma$ pair the deviation of its effective mass from the π^0 mass, $\Delta M(\gamma\gamma) = M(\gamma\gamma) - m(\pi^0)$, is calculated. If this deviation is in the range of $|\Delta M(\gamma\gamma)| < 50$ MeV, the $\gamma\gamma$ pair is considered as a candidate of the π^0 decay. Then, if this $\gamma\gamma$ pair is taken as a π^0 decay, the four-momenta of its photons are multiplied by a factor $\lambda = m(\pi^0)/M(\gamma\gamma)$. The π^0 detection is illustrated in Fig. 2, where the spectrum of the effective masses of the "best" $\gamma\gamma$ pairs, i.e. the pairs with the smallest value of $|\Delta M(\gamma\gamma)|$, is shown separately for the selected events with four and three detected photons. In further selections all combinatorial π^0 candidates are used, not only the "best".

In the third step of the event selection two samples are collected: 1) the $K^- \to \pi^-\gamma\gamma\gamma\gamma$ events with two $\pi^0 \to \gamma\gamma$ decays and 2) the $K^- \to \pi^-\gamma\gamma\gamma(\gamma)$ events with one $\pi^0 \to \gamma\gamma$ decay and with the single photon (the fourth photon, denoted in the parentheses, is not detected).

For the first sample the further selection is done by the requirements that the measured value of the kaon mass is in the range of $|M(\pi^-\pi^0\pi^0) - m(K^-)| < 80$ MeV (see Fig. 3) and then the event passes the kinematical 6C-fit for the $K^- \to \pi^-\pi^0\pi^0$ hypothesis. The efficiency of the last cut is about 72%. Both requirements are considered for all possible combinations of photons and the best 6C-fit hypothesis is chosen.

For the second sample some additional variables are used. They are given in the decay notation re-written as $K^- \to \pi^-\pi^0 X$, where π^0 is the chosen candidate of the $\pi^0 \to \gamma\gamma$ decay and $X \to \gamma(\gamma)$ is the system containing the single photon and having the four-momentum $p(X) = p(K^-) - p(\pi^-\pi^0)$. The further selection is done by the requirements

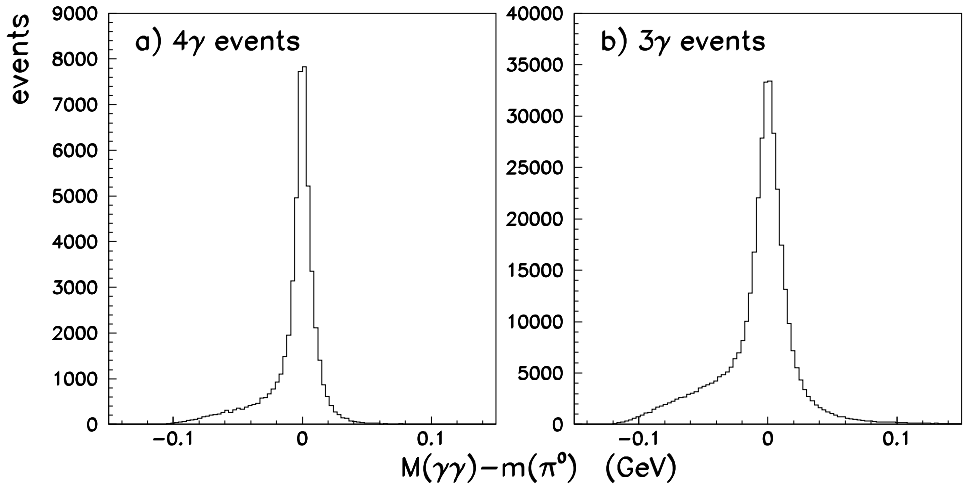

Figure 2: The deviation $\Delta M(\gamma\gamma) = M(\gamma\gamma) - m(\pi^0)$ of the effective mass of the $\gamma\gamma$ pair with the smallest value of $|\Delta M(\gamma\gamma)|$ in the selected events with **a)** four and **b)** three detected photons.

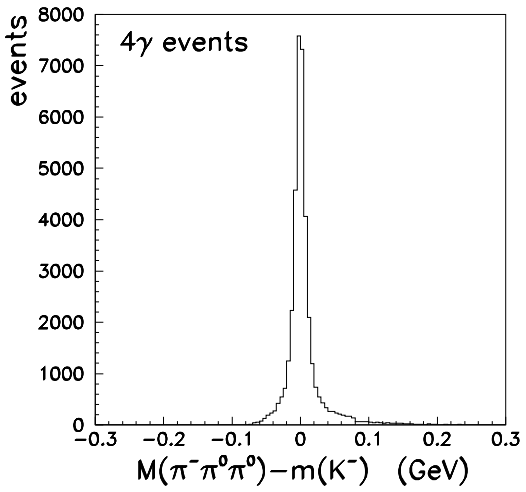

Figure 3: The deviation of the effective mass of the $\pi^-\pi^0\pi^0$ system from $m(K^-)$ in the selected events with four detected photons.

that the value of the missing mass $M(X)$ is in the range of $|M(X) - m(\pi^0)| < 80$ MeV (see Fig. 4a) and then the energy of the single photon in the rest frame of the system X is in the range of $|E^\star_X(\gamma) - \frac{1}{2}m(\pi^0)| < 70$ MeV (see Fig. 4b). To remove the other surviving

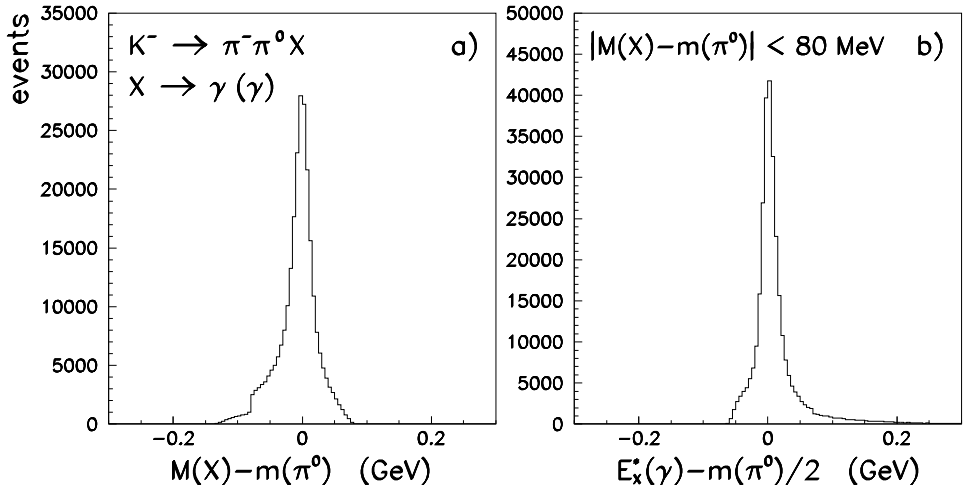

Figure 4: **a)** The deviation from $m(\pi^0)$ of the missing mass to the $\pi^-\pi^0$ system and **b)** the deviation from $\frac{1}{2}m(\pi^0)$ of the energy of the single photon in the rest frame of the missing system X having the mass in the range of $|M(X) - m(\pi^0)| < 80$ MeV. Both distributions are given for the selected events with three detected photons.

modes of the kaon decay the values of the total energy in the beam rest frame $E^\star_{tot}$ are calculated for the following hypotheses: $K^- \to \pi^-\pi^0$, $K^- \to \pi^-\pi^0(\pi^0)$, $K^- \to \mu^-\pi^0(\bar{\nu}_\mu)$ and $K^- \to e^-\pi^0(\bar{\nu}_e)$, assuming that only the secondary charged particle and one π^0 meson are detected (the particle denoted in the parentheses is not detected). If the hypothesis with the smallest value of $\Delta E^\star_{tot} = |E^\star_{tot} - m(K^-)|$ is not the $K^- \to \pi^-\pi^0(\pi^0)$ decay, it is removed from the second sample when $\Delta E^\star_{tot} < 50$ MeV. Finally, the event is selected if it passes the kinematical 3C-fit for the $K^- \to \pi^-\pi^0\pi^0$ hypothesis. The efficiency of this last cut is about 78%. All selection criteria are considered for all possible combinations of photons and the best 3C-fit hypothesis is chosen.

Using the mentioned above selection criteria we have collected for the $K^- \to \pi^-\pi^0\pi^0$ decay the following numbers of events: 26K events with four detected photons and 188K events with three detected photons. The corresponding numbers of accepted Monte Carlo events are about four times larger than in the experiment. The surviving background is estimated from the Monte Carlo simulation to be less than 0.3% for the first sample and less than 1% for the second sample.

The detailed event reduction statistics is given in Table 1.

4 Analysis

To determine the parameters g, h and k in Eq. (1) the distribution $\rho(X, Y)$ of the event density on the Dalitz plot was analyzed. This distribution is shown in Fig. 5 separately for the selected events with four and three detected photons. At first the background contamination was subtracted from the Dalitz plot. The contamination was estimated from the Monte Carlo simulation of the particle interaction with the material of the

Table 1: The event reduction statistics for the 1999 and 2001 runs.

Run	*1999*	*2001*
Total number of events	206 M	363 M
Beam track reconstructed	159 M	269 M
Secondary tracks reconstructed	81 M	134 M
Number of events written on DST	57 M	90 M
K^- and π^- selected (all cuts of the 1st step)	5458 K	7311 K
at least one π^0 selected (all cuts of the 2nd step)	733 K	771 K
$\pi^-\pi^0\pi^0$ selected in 3γ events before 3C-fit	121 K	121 K
$\pi^-\pi^0\pi^0$ selected in 4γ events before 6C-fit	18 K	19 K
$\pi^-\pi^0\pi^0$ selected in 3γ events after 3C-fit	95 K	93 K
$\pi^-\pi^0\pi^0$ selected in 4γ events after 6C-fit	13 K	13 K

detector and of the kaon decay including all decay modes with the branching ratios more than 1%. The corresponding branching ratios and matrix elements in this simulation were taken from the PDG [11]. In Fig. 6 the fraction of the background contamination is shown as functions of the Dalitz plot variables $|X|$ and Y.

The background subtracted distribution $\rho'(X,Y)$ was fitted by the method of least squares with the function:

$$\rho'(X,Y) \;\propto\; F_1(X,Y) + g\,F_2(X,Y) + h\,F_3(X,Y) + k\,F_4(X,Y), \tag{3}$$

where $F_k(X,Y)$ are the distributions of the w_k–weighted Monte Carlo $K^- \to \pi^-\pi^0\pi^0$ events generated with the constant matrix element and reconstructed with the same program as for the real events. The weight factors $w_1 = 1$, $w_2 = Y_{true}$, $w_3 = Y^2_{true}$ and $w_4 = X^2_{true}$ are given by the "true" values of X and Y, but the bins of $F_k(X,Y)$ are given by the "measured" ones. This method allows to avoid the systematic errors [12] due to the "migration" of the events on the Dalitz plot because of the finite experimental resolution. Fig. 7 illustrates the Monte Carlo estimated experimental resolution for the variables $|X|$ and Y, where the "measured" values are shown versus the "true" ones.

5 Results

The result of the least squares fit is illustrated in Fig. 8, where the matrix element

$$|A(K^- \to \pi^-\pi^0\pi^0)|^2 \;=\; C \cdot \frac{\rho'(X,Y)}{F_1(X,Y)} \tag{4}$$

for the $K^- \to \pi^-\pi^0\pi^0$ events with at least three detected photons is shown as a function of Y in the different intervals of $|X|$. The normalization constant C in Eq. (4) provides

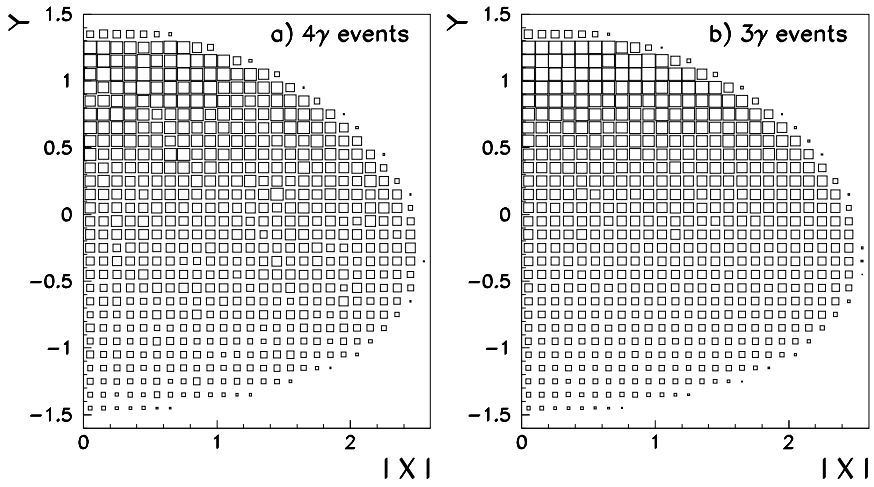

Figure 5: The Dalitz plot, $Y = (s_3 - s_0)/m_\pi^2$ *versus* $X = (s_1 - s_2)/m_\pi^2$, for the selected $K^- \to \pi^-\pi^0\pi^0$ events with **a)** four and **b)** three detected photons.

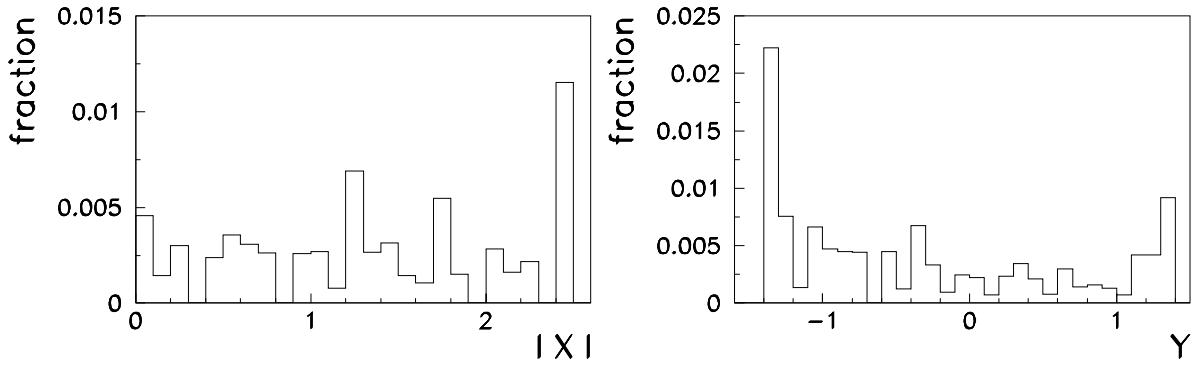

Figure 6: The fraction of the background contamination as a function of the Dalitz plot variable.

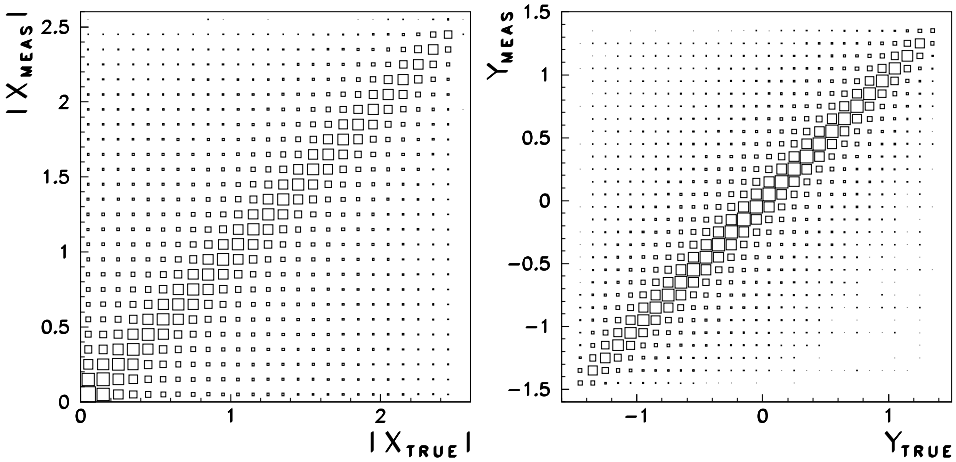

Figure 7: The "measured" values of the Dalitz plot variables $|X|$ and Y versus the "true" ones estimated from the Monte Carlo simulation.

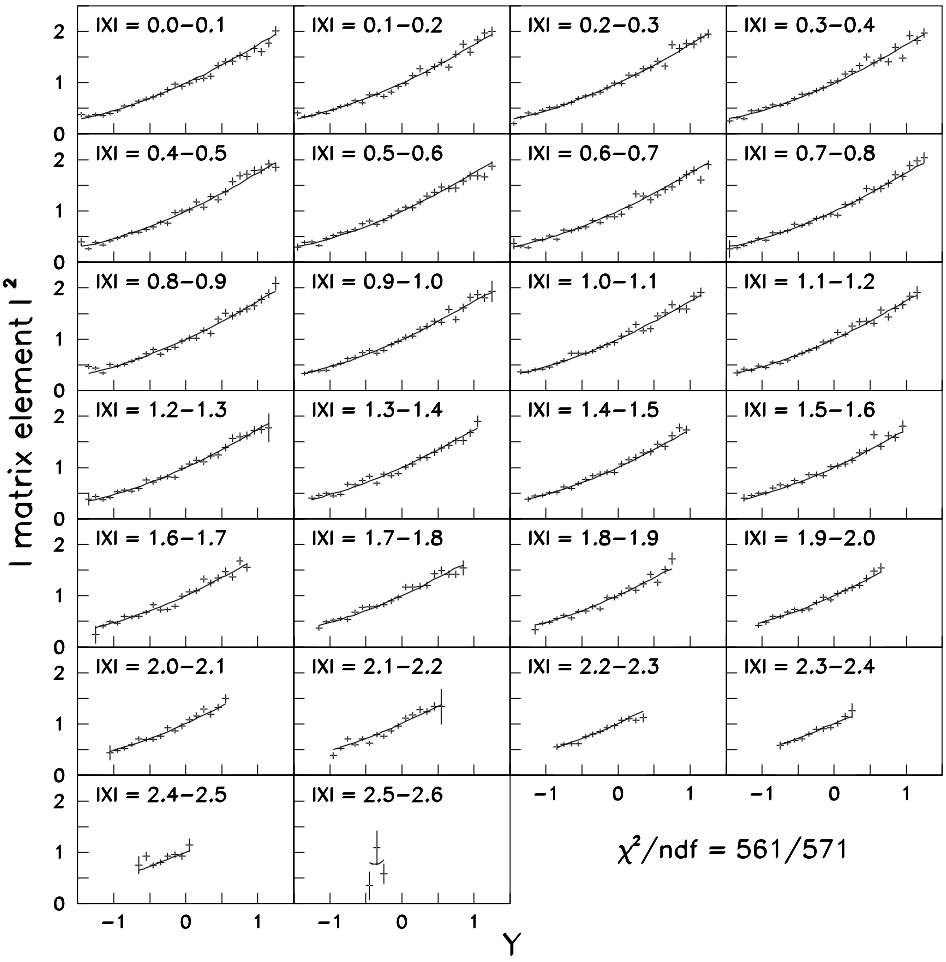

Figure 8: The matrix element dependence on the variable Y in the different intervals of the variable $|X|$ for the $K^- \to \pi^-\pi^0\pi^0$ events with at least three detected photons. The curves are the result of the fit to the function (3).

the value of $|A|^2 = 1$ at the point (X=0, Y=0). The integrated dependences of the matrix element on the variables Y and $|X|$ are shown in Fig. 9.

The values of the Dalitz plot slope parameters are found to be

$$\begin{aligned} g &= 0.697 \pm 0.007 \pm 0.019, \\ h &= 0.124 \pm 0.007 \pm 0.035, \\ k &= 0.006 \pm 0.002 \pm 0.004 \end{aligned}$$

with $\chi^2/ndf = 561/571$ for the sample of the events with at least three detected photons and

$$\begin{aligned} g &= 0.709 \pm 0.016 \pm 0.014, \\ h &= 0.105 \pm 0.015 \pm 0.030, \\ k &= 0.002 \pm 0.004 \pm 0.004 \end{aligned}$$

with $\chi^2/ndf = 627/559$ for the sample of the events with four detected photons. Here the first errors are statistical and the second ones are systematic.

In the determination of the systematic errors of the slope parameters measurement the following contributions were taken into account.

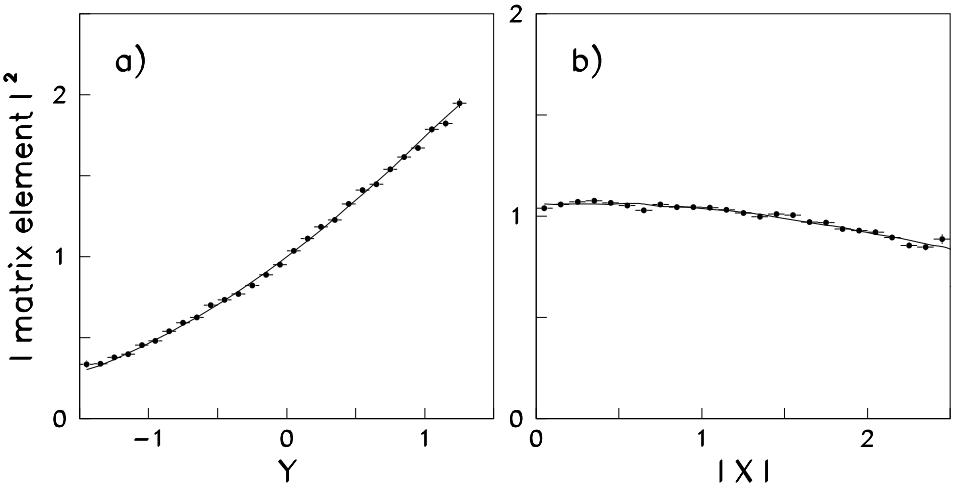

Figure 9: The integrated dependences of the matrix element on the variables **a)** Y and **b)** $|X|$ for the selected $K^- \to \pi^-\pi^0\pi^0$ events with at least three detected photons. The curves are the result of the fit to the function (3).

– Two samples of the events collected in the runs (1999 and 2000) with some differences in characteristics of the setup were fitted separately (the corresponding contribution to the systematic error is $\Delta g = 0.007$).

– To avoid some uncertainties at the edge of the Dalitz plot the extreme bins of this plot were cut ($\Delta g = 0.009$).

– The energy threshold of the selected photons was increased from the value of 0.7 GeV to 2 GeV ($\Delta g = 0.010$).

– The mass and energy ranges used in the event selection criteria were varied from the value of 30 MeV to 80 MeV ($\Delta g = 0.004$).

– The background contamination estimated from the Monte Carlo simulation was not subtracted from the Dalitz plot before the least squares fit ($\Delta g = 0.010$).

6 Summary and conclusion

The Dalitz plot slope parameters for the $K^- \to \pi^-\pi^0\pi^0$ decay have been measured using the "ISTRA+" spectrometer. The results of our measurement, the world averages [11] and the results of previous experiments [6, 7, 13 – 19] on the $K^\pm \to \pi^\pm\pi^0\pi^0$ decays are presented in Fig. 10. Among the previous experiments there are eight measurements of the K^+ decay, but only one of the K^- decay. Our values of the slope parameters g and h are consistent with the world averages dominated by K^+ measurements. The difference between the values of the linear slope g obtained for the $K^- \to \pi^-\pi^0\pi^0$ decay in our experiment and in another one [7] is 3.9 standard deviations.

One can obtain, including our measurement and using the same rules as in the PDG [11], the world average values of the linear slope g for the K^+ and K^- decays separately: $g^+ = 0.672 \pm 0.030$ and $g^- = 0.642 \pm 0.057$. They give for the charge asymmetry (2) the value of $(\delta g)_{\tau'} = 0.02 \pm 0.05$.

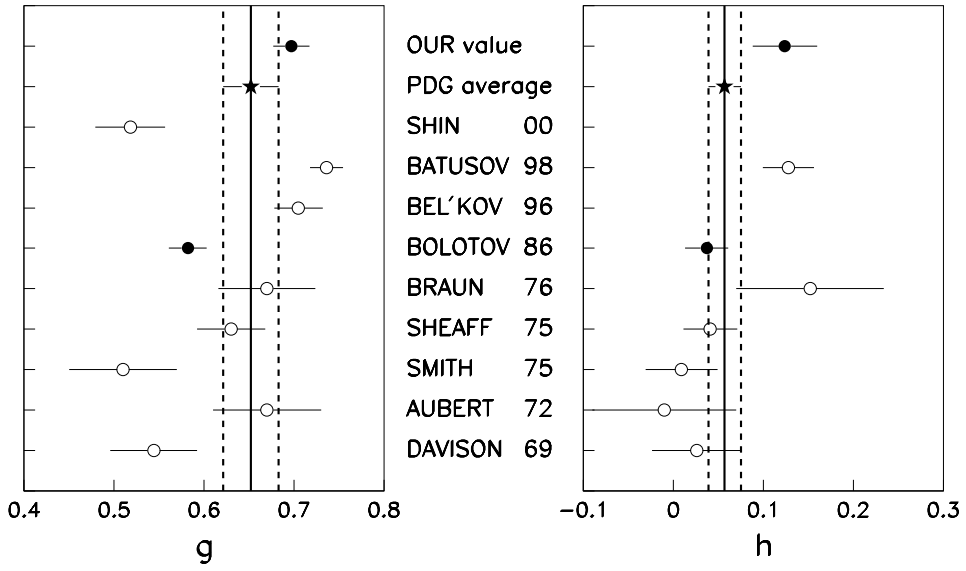

Figure 10: The Dalitz plot slope parameters g and h for the $K^- \to \pi^-\pi^0\pi^0$ (solid circles), $K^+ \to \pi^+\pi^0\pi^0$ (open circles) and $K^\pm \to \pi^\pm\pi^0\pi^0$ (solid stars) decays.

References

[1] G. D'Ambrosio, G. Isidori, *Int. J. Mod. Phys.*, **A13** (1998) 1.

[2] L. Maiani, N. Paver, In *The 2nd DAΦNE Physics Handbook (eds. L. Maiani et al.)*, vol. 1, p. 51, INFN–LNF, Frascati, 1995;
A.A. Bel'kov et al., *Phys. Lett.*, **B232** (1989) 118.

[3] G. D'Ambrosio, G. Isidori, G. Martinelli, *Phys. Lett.*, **B480** (2000) 164.

[4] S. Weinberg, *Phys. Rev. Lett.*, **37** (1976) 657.

[5] E. Shabalin, Preprint ITEP 8-98, 1998.

[6] V.Y. Batusov et al., *Nucl. Phys.*, **B516** (1998) 3.

[7] V.N. Bolotov et al., *Sov. J. Nucl. Phys.*, **44** (1986) 73.

[8] V.N. Bolotov et al., Preprint IHEP 95-111, Protvino, 1995.

[9] I.V. Ajinenko et al., Preprint IHEP 2001-51, Protvino, 2001;
I.V. Ajinenko et al., Preprint IHEP 2002-06, Protvino, 2002.

[10] R. Brun et al., Preprint CERN-DD/EE/84-1.

[11] *Particle Data Group*, D.E. Groom et al., *Eur. Phys. J.*, **C15** (2000) 1.

[12] V.B. Anikeev, V.P. Zhigunov, *Phys. Part. Nucl.*, **24** (1993) 989.

[13] D. Davison et al., *Phys. Rev.*, **180** (1969) 1333.

[14] B. Aubert et al., *Nuovo Cim.*, **12A** (1972) 509.

[15] K.M. Smith et al., *Nucl. Phys.*, **B91** (1975) 45.

[16] M. Sheaff, *Phys. Rev.*, **D12** (1975) 2570.

[17] H. Braun et al., *Lett. Nuovo Cim.*, **17** (1976) 521.

[18] A. Bel'kov et al., In *Proc. of the 28th Int. Conf. on High Energy Physics (Warsaw, 1996)*, vol. 2, p. 1204, eds. Z. Ajduk and A.K. Wroblewski, World Scientific, 1997.

[19] Y.-H. Shin et al., *Eur. Phys. J.*, **C12** (2000) 627.